

Formation of ultrashort pulses from quasimonochromatic XUV radiation via infrared-field-controlled forward scattering

T. R. Akhmedzhanov,^{1,*} V. A. Antonov,^{2,3,4} and Olga Kocharovskaya¹

¹*Department of Physics and Astronomy and Institute for Quantum Studies and Engineering, Texas A&M University, College Station, Texas 77843-4242, USA*

²*Institute of Applied Physics of the Russian Academy of Sciences, 46 Ulyanov Street, Nizhny Novgorod 603950, Russia*

³*N. I. Lobachevsky State University of Nizhny Novgorod, 23 Gagarin Avenue, Nizhny Novgorod 603950, Russia*

⁴*Kazan Federal University, 18 Kremlyovskaya Street, Kazan 420008, Republic of Tatarstan, Russia*

(Received 12 April 2016; published 10 August 2016)

We suggest a highly efficient method of ultrashort pulse formation from resonant XUV radiation due to sub-laser-cycle modulation of the excited state of non-hydrogen-like atoms by a nonionizing IR laser field. This modulation results in formation of the Raman-Stokes and anti-Stokes sidebands in coherently forward-scattered radiation, which, in turn, leads to formation of short pulses, when the phases of the sidebands are matched. This method is a generalization of a recently suggested technique [V. A. Antonov *et al.*, *Phys. Rev. A* **88**, 053849 (2013)] for a non-hydrogen-like medium. The possibility to form 2-fs XUV pulses in the gas of helium atoms and 990-as XUV pulses in the plasma of Li⁺ ions with efficiencies over 80% is shown.

DOI: [10.1103/PhysRevA.94.023821](https://doi.org/10.1103/PhysRevA.94.023821)

I. INTRODUCTION

Subfemtosecond XUV pulses provide a unique combination of high spatial and time resolution and find numerous applications to capture the motion of electrons, atoms, and molecules in real time; to observe element-specific dynamics at the *M*- and *L*-shell absorption edges of magnetic materials; etc. [1–6]. The conventional way of producing such ultrashort XUV pulses in a tabletop setup is high-harmonic generation (HHG) in gases [7,8]. This method allows formation of very short pulses (up to 67 as [9]). However, the efficiency of conversion of visible or IR laser radiation into high harmonics is low. In particular, in the water window 2.3–4.4 nm, it is $10^{-8} - 10^{-9}$ [10,11]. It results in low total energy of the generated pulse trains (on the order of nanojoules) which limits their applications. Much higher energy per pulse can be achieved at X-ray free electron lasers (XFELs) in the few-femtosecond regime, but there are only a few such facilities in the world [12–15]. Modern tabletop x-ray lasers are able to generate high-energy (in the millijoule range) x-ray pulses, but with relatively long duration in the range of a few picoseconds [16–18]. Thus, a highly efficient method of transformation of an output pulse of x-ray laser into the subfemtosecond pulses would be very desirable.

Recently, a technique for production of ultrashort pulses from quasimonochromatic XUV radiation via resonant interaction with atoms, dressed by a moderately strong IR laser field, was suggested [19,20] and studied [21–23]. The two regimes of pulse formation were considered: (i) via the linear Stark effect in a hydrogenlike medium, irradiated by the nonionizing IR field, and (ii) via rapid excited-state ionization in arbitrary atomic gas. In the first case, the pulses formation relies on adiabatic (quasistatic) splitting of the resonant excited atomic energy level in space and time due to the linear ac Stark effect. Namely, under the action of the modulating field the instantaneous values of transition frequencies from

the ground to excited energy levels linearly depend on the instantaneous value of the modulating field at the considered moment of time and point in space. The degeneracy of the first excited energy level of hydrogen (or a hydrogenlike ion) and the antiphase shift of its relevant sublevels under the action of the IR field play a key role in the pulses formation. The second regime is based on sudden interruption of the resonant interaction of the XUV field with the medium due to the complete atomic ionization from the resonant excited state within each half cycle of the IR field. In this case, the produced pulses are extremely short. However, since the pulses formation is essentially based on ionization, this regime cannot be realized in the active media of x-ray plasma lasers. Besides, its efficiency is essentially lower than that in the first, nonionizing regime, which is characterized by the very high efficiency of transformation of incident XUV radiation into the ultrashort pulse trains (close to unity) and can be potentially realized in the active media of x-ray lasers. However, since it essentially relies on the degeneracy of the first excited state of hydrogenlike atoms, the possibility of its generalization and realization in the other atomic gases remains questionable.

In the present paper we suggest the generalization of the technique, based on modulation of the resonant excited atomic state by the nonionizing IR field. This approach is not restricted to the atoms of hydrogen and hydrogenlike ions with degenerate excited energy levels. Below, we consider its implementation in the medium of helium or heliumlike ions, but it can be realized in a variety of atomic gases, which makes its experimental realization more feasible and promising for wider potential applications. By using Floquet formalism [24], we study the formation of a train of ultrashort pulses from quasimonochromatic XUV radiation in the gas of IR-field-dressed He atoms. We investigate the case of a not too strong IR field, when the role of ionization is negligible in comparison with mixing and modulation of the excited atomic states. Under the action of IR field the excited states of atoms are properly described in the Floquet basis [24], rather than in the bare one. It is shown that the parameters of the IR field can be optimized in a way such that one

*Corresponding author: timik10f@tamu.edu

of the Floquet states produces a few in-phase sidebands of an incident field with comparable amplitudes. If the incident XUV field is tuned in resonance with this state, the scattered XUV field contains a few sidebands in phase with each other, which, after attenuation of an incident spectral component to the level of generated sidebands, leads to formation of a train of ultrashort pulses. Firstly, within a three-level model of the He atom, we show that the pulses with a time duration of 2 fs can be produced at the output of an optically thin medium of He atoms. Secondly, we verify that neither the presence of higher-lying discrete excited states nor ionization affect the possibility of pulses formation. Thirdly, we consider the propagation problem and show that the efficiency of transformation of an incident quasimonochromatic XUV field into the train of femtosecond pulses in the optically thick medium of helium may exceed 80%. Finally, we show that with proper scaling of the parameters of an IR field, the suggested method allows formation of the train of subfemtosecond pulses in the plasma of He-like ions with an efficiency of 87.4%.

The paper is structured as follows. In Sec. II, we analyze the spectral and temporal properties of the XUV field scattered by an optically thin layer of He atoms within a three-level approximation, using the Floquet approach [24]. We show that for the properly chosen dressing IR field wavelength and intensity, a train of ultrashort pulses can be produced at the output of the medium. In Sec. III, we study the influence of the higher-lying excited states and ionization from the excited states on the pulses formation. At first, we consider a five-level model of He and show that taking into account the two extra excited states does not change the pulse shape appreciably. After that we confirm the possibility of the pulses formation by solving the full time-dependent Schrödinger equation (TDSE), taking into account all the bound and continuum states of an atom in a single active electron approximation. In Sec. IV we numerically study the propagation of an XUV field in the optically thick medium and demonstrate high efficiency of transformation of the incident radiation into the train of ultrashort pulses. In Sec. V we discuss a possibility to reduce the pulse duration using plasma of He-like ions and derive the scaling law which immediately allows finding the IR field parameters required for pulse formation in He-like media. In conclusion we summarize the main results of the paper. Atomic units are used throughout the paper, unless specified otherwise.

II. THREE-LEVEL MODEL

Let us consider the linearly polarized quasimonochromatic XUV radiation, propagating along the x axis through the atomic gas with quasiresonant atomic transition from the ground state, $|1\rangle$, to an excited state, $|2\rangle$. At the input of the medium ($x = 0$), the field is given by

$$\vec{E}(x, t) = \vec{z}_0 \frac{1}{2} \tilde{E}(x, t) \exp\{-i\omega\tau\} + \text{c.c.}, \quad (1)$$

where \vec{z}_0 is the unit vector directed along the polarization of the field, $\tilde{E}(x, t)$ is the amplitude of the field, ω is its carrier frequency, c is the speed of light in vacuum, and c.c. stands for complex conjugation. $\tau = t - x/c$ is the local time in the reference frame, comoving with the x-ray radiation wave. The XUV field is considered to be sufficiently weak so that it does not change the population of the ground and excited states

during the interaction time. We consider an interaction of the XUV field with the atomic gas in the presence of an additional linearly polarized IR field, propagating in the same direction as the XUV radiation:

$$\vec{E}_{\text{IR}}(x, t) = \vec{z}_0 \tilde{E}_{\text{IR}} \cos(\omega_{\text{IR}} \tau), \quad (2)$$

where \tilde{E}_{IR} is the amplitude of the IR field, and ω_{IR} is its frequency. The IR field is moderately strong: It does not couple the ground state to the excited states, but it couples the state $|2\rangle$ to another excited state, $|3\rangle$.

Mixing of the states $|2\rangle$ and $|3\rangle$ by the IR field leads to the appearance of two Floquet states [24]. The wave function of the IR-field-dressed atom can be represented in the Floquet basis as follows [25]:

$$|\psi\rangle = c_1 |1\rangle + \sum_{i=1,2} c_{\lambda_i} \exp(-i\lambda_i \tau) |\Phi_{\lambda_i}(\tau)\rangle, \quad (3)$$

where the energy of the ground state is chosen to be zero. Here λ_i is the quasienergy of the i th Floquet state $|\Phi_{\lambda_i}\rangle$, which periodically depends on time and constitutes the Fourier series:

$$|\Phi_{\lambda_i}(\tau)\rangle = \sum_{m=-\infty}^{+\infty} \exp(-im\omega_{\text{IR}} \tau) \sum_{\alpha} a_m^{i;\alpha} |\alpha\rangle, \quad (4)$$

and c_{λ_i} is an amplitude of this Floquet state. The amplitudes $a_m^{i;\alpha}$ of the Fourier components of the Floquet states (4) and the quasienergies λ_i of these states are determined by the intensity and the frequency of the IR field and can be expressed analytically in terms of the infinite continued fractions (see, e.g., [26]). In the general case $a_m^{i;\alpha}$ are the complex numbers. For the field (2) they can be chosen to be real. The index α enumerates the excited states of a bare atom (an atom in the absence of the IR field), that is, $|2\rangle$ and $|3\rangle$ states. It is worth noting that the quasienergy of the Floquet state is defined up to the integral number of ω_{IR} since the Floquet state $|\Phi_{\lambda_i - n\omega_{\text{IR}}}(\tau)\rangle = \sum_{m=-\infty}^{+\infty} \exp[-i(m+n)\omega_{\text{IR}} \tau] \sum_{\alpha} a_m^{i;\alpha} |\alpha\rangle$ with quasienergy $\lambda_i - n\omega_{\text{IR}}$ is physically the same as the state $|\Phi_{\lambda_i}(\tau)\rangle = \sum_{m=-\infty}^{+\infty} \exp(-im\omega_{\text{IR}} \tau) \sum_{\alpha} a_m^{i;\alpha} |\alpha\rangle$ with quasienergy λ_i [24]. In the following we choose the quasienergies in a way that $m = 0$ corresponds to the levels, nearest to the unperturbed energy of the $1s2p$ state. Another important property of Floquet states is that coefficients $a_m^{i;2}$ are not zeros only for even m , and $a_m^{i;3}$ are not zeros only for odd m (or vice versa—depending on the choice of the quasienergy) [24,25,27], that is, with our choice of quasienergies, $a_{2m+1}^{i;2} = 0$ and $a_{2m}^{i;3} = 0$.

If the XUV field is tuned close to the exact resonance with the transition from the ground state $|1\rangle$ to the only step with $m = k$ of the Floquet state i , then, within the framework of perturbation theory, the slowly varying amplitude of the XUV field at the output of an optically thin medium can be found as [25,27]

$$\begin{aligned} \tilde{E}(x, t) &= \tilde{E}(0, t) + \tilde{E}_{\text{Scatt}} \\ &= \tilde{E}(0, t) - x \frac{2\pi\omega N |d_{2,1}|^2}{c\hbar} \\ &\quad \times e^{-i(\lambda_i - \omega)\tau} \left[\sum_{m=-\infty}^{+\infty} a_{2m}^{i,2} \exp(-2im\omega_{\text{IR}} \tau) \right] \\ &\quad \times \int_{-\infty}^{\tau} \exp[i(\lambda_i - \omega)\tau'] \tilde{E}(\tau') (a_k^{i,2})^* d\tau'. \end{aligned} \quad (5)$$

Excitation of another Floquet state by the XUV field is negligible as long as the bandwidth of the incident XUV pulse is small as compared to the frequency separation between the two neighboring Floquet states (i.e., the pulse duration is sufficiently large). As it is seen from (5), the properties of the output field are controlled by the amplitudes $a_{2m}^{i:2}$ of the Fourier components of the Floquet states, which are determined by the parameters of the IR field. In order to form a train of ultrashort pulses we need to find the wavelength and intensity of the IR field that correspond to a Floquet state where the majority of coefficients $a_{2m}^{i:2}$ will have comparable amplitudes and nearly the same phases. Within the framework of Hermitian Floquet theory, this optimization can be quickly done numerically for some specific atom. The $a_{2m}^{i:2}$ are determined by the two dimensionless parameters, namely, by the ratios of the IR field frequency, ω_{IR} , and the Rabi frequency of the IR field, $\tilde{E}_{\text{IR}}d_{2,3}$ (where $d_{2,3}$ is the dipole moment of transition $|2\rangle \leftrightarrow |3\rangle$), to the frequency of transition $|2\rangle \leftrightarrow |3\rangle$; those are $\omega_{\text{IR}}/\omega_{23}$ and $\tilde{E}_{\text{IR}}d_{2,3}/\omega_{23}$.

Let us consider, in particular, a gas of helium atoms under the following conditions. The XUV field is weak and its frequency is close to the frequency of transition from the ground state $1s^2$ to the $1s2p$ state. So it couples only these states, exciting polarization at the transition $1s^2 \leftrightarrow 1s2p$. The IR field is low frequency (as compared to the frequencies of transitions from the resonantly populated $1s2p$ state to the other states of helium) and not too strong. Taking into account that the dipole moment of transition $1s2s \leftrightarrow 1s2p$ is a few times larger than those of transitions from the resonant $1s2p$ state to the other excited states, while the frequency of transition $1s2s \leftrightarrow 1s2p$ is a few times smaller, it is reasonable to consider coupling of the IR field only to the $1s2s \leftrightarrow 1s2p$ transition. The corresponding transition wavelengths are shown in Fig. 1(a). Thus, the three-level model, including the $1s^2$, $1s2s$, and $1s2p$ states (which are

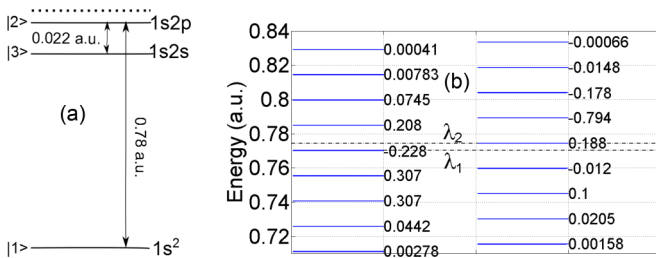


FIG. 1. (a) Three-level model and its implementation in helium. Vertical arrows correspond to the transition wavelengths. Transition energies are shown in atomic units. (b) Coupling of $1s2s$ and $1s2p$ states of He by the IR field leads to formation of the two Floquet states. Each state corresponds to the energy ladder with the steps separated by the IR field frequency. However, the steps containing the same state ($|2\rangle$ or $|3\rangle$) are separated by the doubled photon energy of the IR field. Only the steps containing the $2p$ state are shown. Note that these steps do not contain the $2s$ state, since $a_{2m}^{i:2s} = 0$ (vice versa, the steps containing the $2s$ state do not contain the $2p$ state, since $a_{2m+1}^{i:2p} = 0$, and hence they are not coupled to the XUV field). The vertical axis corresponds to energy in atomic units, while numbers near the steps correspond to the amplitudes $a_{2m}^{i:2p}$. The quasienergies λ_1 and λ_2 are shown by the dashed black horizontal lines. The IR field parameters are $\lambda = 6176$ nm, $I = 2.5 \times 10^{12}$ W/cm².

the states $|1\rangle$, $|3\rangle$, and $|2\rangle$ in our notation, correspondingly) is well justified in the case under consideration (the role of other excited discrete states and continuum will be investigated in the next sections).

As it was already mentioned, mixing of $1s2s$ and $1s2p$ states by the IR field leads to the appearance of two Floquet states. We optimize the IR field parameters in order for one of the Floquet states to have a few $a_{2m}^{i:2p}$'s of the same phase and comparable amplitudes. The result of optimization is shown in Fig. 1(b). As it can be seen, the first Floquet state [the left ladder in Fig. 1(b)] contains six sidebands of the same order of magnitude, with five of them having the same sign. The IR field producing this Floquet state has a wavelength of 6176 nm (corresponding to $\omega_{\text{IR}}/\omega_{23} \approx 1/3$) and intensity $I = 2.5 \times 10^{12}$ W/cm² (corresponds to $\tilde{E}_{\text{IR}}d_{23}/\omega_{23} \approx 1.11$).

The spectral structure of the resonantly scattered field is fully defined by the structure of the Floquet ladder itself. However, the XUV radiation at the output of an optically thin medium is a sum of the incident and scattered fields. In an absorbing medium, the resonant component of the scattered field is always in antiphase to the incident field. Therefore, if the resonant component is in antiphase to the others, then all the other spectral components will be in phase with the incident XUV field, resulting in pulses formation, while if the resonant component is in phase with the others, then most of the sidebands will be in antiphase with the incident field, and the pulses will not be produced. Thus, the XUV field should be tuned in resonance with the step of the Floquet ladder with $a_2^{1:2p} = -0.228$, which has the opposite sign in comparison to the other steps. In the considered case, it corresponds to a wavelength of 59.16 nm. It is worth noting that in general, when the excited-state ionization is taken into account, the quasienergies λ_i are complex numbers [24]. In order to take into account the finite lifetime of the excited states $|2\rangle$ and $|3\rangle$ within the three-level model, we add a small complex part γ_i to both λ_1 and λ_2 , $\gamma_i \ll \omega_{\text{IR}}$, $|\lambda_1 - \lambda_2|$, artificially. The value γ_i determines the half linewidths of transitions to the ground atomic state, $|1\rangle \leftrightarrow |2\rangle$ and $|1\rangle \leftrightarrow |3\rangle$. In turn, the bandwidth of an incident XUV field is considered to be smaller than this linewidth. Under such conditions the XUV field, scattered by atoms under the simultaneous action of monochromatic XUV and IR fields, is given by

$$\tilde{E}_{\text{scatt}} = -x A \tilde{E}_0 \frac{a_2^{1,2p}}{\gamma} \left[\sum_m a_{2m}^{1,2p} \exp(-2im\omega_{\text{IR}}\tau) \right], \quad (6)$$

where $A = \frac{2\pi\omega N|d_{2p1s}|^2}{c\hbar}$ and \tilde{E}_0 is the incident XUV field amplitude. The validity of these assumptions is justified in the next sections via numerical solution of the full TDSE. The spectral structure of this field corresponds to the Floquet ladder on the left of in Fig. 1(b). The XUV radiation at the output of the thin medium is given by the sum of the scattered field and the incident field:

$$\begin{aligned} \tilde{E}(x,t) &= \tilde{E}_0 - x A \tilde{E}_0 \frac{a_2^{1,2p}}{\gamma} \left[\sum_m a_{2m}^{1,2p} \exp(-2im\omega_{\text{IR}}\tau) \right] \\ &\approx \tilde{E}_0 - x \tilde{E}_0 A \frac{a_2^{1,2p}}{\gamma} \left[\sum_{m \neq 0} a_{2m}^{1,2p} \exp(-2im\omega_{\text{IR}}\tau) \right]. \end{aligned} \quad (7)$$

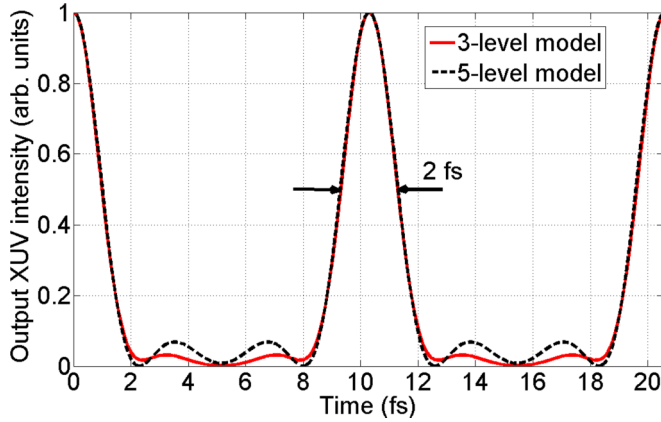


FIG. 2. Intensity of the 59.16-nm XUV field at the exit of an optically thin layer of helium, irradiated by a 6176-nm IR field with intensity $I = 2.5 \times 10^{12} \text{ W/cm}^2$. The solid red line corresponds to the three-level model, dashed black line corresponds to the five-level model. The incident XUV frequency component is attenuated according to (8).

Summation of the incident and the resonantly scattered fields results in phase matching of the central frequency component with the sidebands. To produce the pulses of shortest duration, the amplitude of the incident XUV field spectral component at the output of the medium should be attenuated to the level of the generated sidebands. In such a case, the output XUV field takes the form

$$\tilde{E}(x, t) = -x A \tilde{E}_0 \frac{a_2^{1,2p}}{\gamma} \left[\sum_{m \neq 0} a_{2m}^{1,2p} \exp(-2im\omega_{\text{IR}}\tau) - a_2^{1,2p} \right]. \quad (8)$$

This field corresponds to the train of well-shaped pulses with pulse duration 2 fs, shown in Fig. 2 by the solid red line. An attenuation can be produced by frequency-selective multilayer mirrors with half of the FWHM of the reflectivity curve less than $2\omega_{\text{IR}}$ [28,29]. On the other hand, it is not necessary to attenuate the incident XUV spectral component with the additional tools. Instead, one may simply increase the optical thickness of the resonant absorbing modulated medium. In the last case, the produced pulses will be slightly longer, but the efficiency of transformation of the incident XUV radiation into the pulse train can exceed 80%. The possible experimental realizations of the last approach are discussed in Secs. IV and V.

It is worth noting that the pulses formation does not require exact tuning of wavelength of the IR and XUV fields, which may vary in the ranges 6100–6200 nm and 59.05–59.25 nm, respectively (although a larger pedestal up to 0.2 of peak pulse intensity might appear).

The choice of modulation field parameters, presented above, is not unique. Namely, the proper Floquet state with comparable amplitudes and nearly the same phases of the spectral components, resulting in ultrashort pulses formation, can be produced with different choices of frequency and intensity of the IR field. For example, in Fig. 3 we show the train of pulses with duration 1.2 fs and carrier wavelength 59.24 nm,

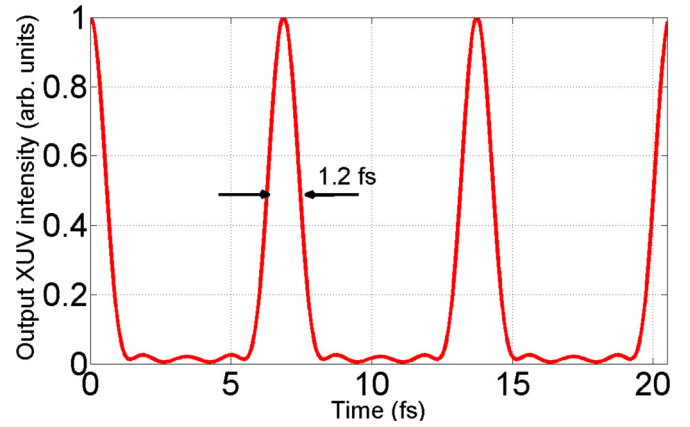


FIG. 3. Intensity of the 59.24-nm field at the exit of an optically thin layer of helium irradiated by a 4117-nm IR field with intensity $I = 8.0 \times 10^{12} \text{ W/cm}^2$. The incident XUV spectral component is attenuated according to (8).

formed in an optically thin layer of helium atoms irradiated by a 4117-nm IR field with intensity $I = 8.0 \times 10^{12} \text{ W/cm}^2$ [the incident XUV spectral component is attenuated according to (8)]. However, in general, with further increase of intensity or shortening of wavelength of the IR field, the three-level approximation becomes invalid, so that more levels need to be taken into account. Moreover, the linewidth of the resonant XUV transition becomes broader due to the increased excited-state-ionization rate, making the selective interaction of the XUV field with only one specific Floquet state impossible.

III. ROLE OF HIGHER-LYING STATES AND IONIZATION

In this section, we study the influence of higher-lying bound energy levels of helium, as well as ionization, on the spectral and temporal properties of the output XUV radiation and prove that the results, derived in the previous section for the three-level model, still hold within more accurate models of the helium atom.

Firstly, we repeat the Floquet-state calculation, taking into account five unperturbed states of the helium atom, namely, $1s^2$, $1s2s$, $1s2p$, $1s3s$, and $1s3d$ states. We have added the $1s3s$ and $1s3d$ states, since they correspond to the strongest dipole-allowed transitions from the $1s2p$ state (with the exception of the $1s2s \leftrightarrow 1s2p$ transition) and are the closest to it in energy. The excited states $1s2s$, $1s2p$, $1s3s$, and $1s3d$ are coupled to each other by the IR field. The IR field with the same parameters as considered in the previous section (wavelength 6176 nm and intensity $I = 2.5 \times 10^{12} \text{ W/cm}^2$) produces four Floquet states. One of these states has amplitudes of the “steps” $a_{2m}^{i:2p}$ ’s, which are very similar to the $a_{2m}^{i:2p}$ ’s of one of the two Floquet states, calculated within the three-level model [the corresponding ladder looks similar to the one on the left in Fig. 1(b)]. Excitation of this state by the resonant XUV field with the wavelength 59.23 nm (which is slightly different from the value 59.16 nm, given by the three-level model) and subsequent attenuation of the incident XUV spectral component to the level of the sidebands according to (8) leads to formation of the ultrashort pulse train shown in Fig. 2 by the dashed black line. As it can be seen, the agreement between

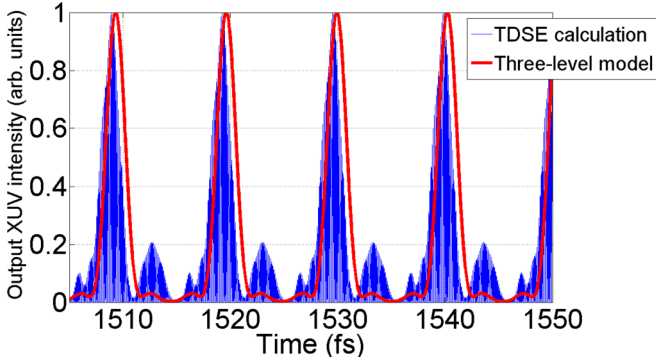


FIG. 4. The results of TDSE calculation. Intensity of the 59.24-nm XUV radiation after propagation through an optically thin medium of helium, irradiated by a 6176-nm IR field with intensity $I = 2.5 \times 10^{12} \text{ W/cm}^2$. The spectral component at the incident XUV radiation frequency is attenuated to the level of the adjacent sidebands.

the predictions of three-level and five-level models is excellent, except for a minor difference in pedestal shape.

Secondly, we study the influence of the higher-lying bound atomic states as well as ionization on pulses formation on the basis of numerical solution of the full TDSE for a helium atom simultaneously interacting with XUV and IR field. We use the numerical scheme first introduced in [30], and the model potential [31]. In order to find the proper frequency of the incident XUV field for TDSE calculation, we firstly repeat the Floquet states calculation within the five-level model with parameters of the states $1s^2$, $1s2s$, $1s2p$, $1s3s$, and $1s3d$, defined by the model potential [31]. The XUV field, quasiresonant to the required Floquet state, has wavelength 59.24 nm. We perform TDSE calculation for He atoms placed in this XUV field along with a 6176-nm IR field with intensity $I = 2.5 \times 10^{12} \text{ W/cm}^2$. As a result, we numerically find the

induced dipole moment $d(t) = \langle z(t) \rangle$. The XUV field at the output of the optically thin medium is given by

$$\tilde{E}_{\text{XUV}}(x, \tau) = \tilde{E}_{\text{XUV}}(0, \tau) - \frac{2\pi x}{c} \frac{dP}{dt}, \quad P = Nd(t). \quad (9)$$

The squared modulus of this field after attenuation of the incident XUV spectral component to the level of the adjacent sidebands is shown in Fig. 4 by the thin blue line. As it can be seen, the pulses are clearly formed and are in a rather good agreement with predictions of the three-level model, shown in Fig. 4 by the bold red line. Thus, the performed calculations confirm the validity of the simple three-level model of He and open up the prospects for experimental realization of the suggested method.

IV. PROPAGATION EFFECTS AND EFFICIENCY OF THE METHOD

In this section we analyze the effects of propagation of the XUV radiation through the optically thick medium of helium, dressed by the IR field, on the shape of produced pulses and determine the efficiency of transformation of the incident XUV radiation into the pulse train.

Propagation of the resonant XUV field through an optically thick gas of helium irradiated by the strong IR field is described by the wave equation for the XUV field and the density matrix equations for the helium atoms. Use of the density matrix allows taking into account both ionization and collisional broadening of the atomic transition lines. Within the previously formulated three-level model, in the slowly varying amplitude approximation for the XUV field and the resonant polarization of the medium, as well as the rotating-wave approximation for the elements of the density matrix, and the approximation of the given amplitude of the IR field, the equations take the form

$$\begin{aligned} \frac{\partial \tilde{E}}{\partial x} &= i \frac{2\pi\omega}{c} \tilde{P} \\ \tilde{P} &= 2Nd_{1s,2p} \tilde{\rho}_{2p,1s} \\ \frac{\partial \tilde{\rho}_{1s,1s}}{\partial \tau} &= -\gamma_{1s} \tilde{\rho}_{1s,1s} + \frac{id_{1s,2p}}{2} (\tilde{E}^* \tilde{\rho}_{2p,1s} - \tilde{E} \tilde{\rho}_{1s,2p}) \\ \frac{\partial \tilde{\rho}_{2s,2s}}{\partial \tau} &= -\gamma_{2s} \tilde{\rho}_{2s,2s} + i \tilde{E}_{\text{IR}} \cos(\omega_{\text{IR}} \tau) d_{2s,2p} (\tilde{\rho}_{2p,2s} - \tilde{\rho}_{2s,2p}) \\ \frac{\partial \tilde{\rho}_{2p,2p}}{\partial \tau} &= -\gamma_{2p} \tilde{\rho}_{2p,2p} - \frac{id_{1s,2p}}{2} (\tilde{E}^* \tilde{\rho}_{2p,1s} - \tilde{E} \tilde{\rho}_{1s,2p}) - i \tilde{E}_{\text{IR}} \cos(\omega_{\text{IR}} \tau) d_{2s,2p} (\tilde{\rho}_{2p,2s} - \tilde{\rho}_{2s,2p}) \\ \frac{\partial \tilde{\rho}_{2p,1s}}{\partial \tau} &= -[\gamma_{2p,1s} + i(\omega_{2p} - \omega)] \tilde{\rho}_{2p,1s} + \frac{id_{1s,2p} \tilde{E}}{2} (\tilde{\rho}_{1s,1s} - \tilde{\rho}_{2p,2p}) + i \tilde{E}_{\text{IR}} \cos(\omega_{\text{IR}} \tau) d_{2s,2p} \tilde{\rho}_{2s,1s} \\ \frac{\partial \tilde{\rho}_{2s,1s}}{\partial \tau} &= -[\gamma_{2s,1s} + i(\omega_{2s} - \omega)] \tilde{\rho}_{2s,1s} - \frac{id_{1s,2p} \tilde{E}}{2} \tilde{\rho}_{2s,2p} + i \tilde{E}_{\text{IR}} \cos(\omega_{\text{IR}} \tau) d_{2s,2p} \tilde{\rho}_{2p,1s} \\ \frac{\partial \tilde{\rho}_{2p,2s}}{\partial \tau} &= -[\gamma_{2p,2s} + i(\omega_{2p} - \omega_{2s})] \tilde{\rho}_{2p,2s} + \frac{id_{1s,2p} \tilde{E}}{2} \tilde{\rho}_{1s,2s} + i \tilde{E}_{\text{IR}} \cos(\omega_{\text{IR}} \tau) d_{2s,2p} (\tilde{\rho}_{2s,2s} - \tilde{\rho}_{2p,2p}), \end{aligned} \quad (10)$$

where $\tilde{\rho}_{ij}$ are the slowly varying amplitudes of the density matrix elements; \tilde{P} is slowly varying atomic polarization; $\omega_{2s,1s} = (E_{2s} - E_{1s})/\hbar$ and $\omega_{2p,1s} = (E_{2p} - E_{1s})/\hbar$ are the

frequencies of transitions $1s2s \leftrightarrow 1s2p$ and $1s^2 \leftrightarrow 1s2p$, respectively; and γ_i and $\gamma_{i,j}$ are decay rates of the diagonal and nondiagonal elements of the density matrix. The population

decay rate γ_i is estimated as the ionization rate from the corresponding i th atomic state under the action of the IR field, which is determined from auxiliary numerical calculation (by numerically solving the time-dependent Schrödinger equation with He model potential [31]). The considered parameters of the IR field are wavelength 6176 nm and intensity $I = 2.5 \times 10^{12}$ W/cm²; $\gamma_{2p} \approx 2 \times 0.11\omega_{\text{IR}}$, $\gamma_{2s} = 2 \times 0.055\omega_{\text{IR}}$, and $\gamma_{1s} \approx 0$. Since in a rare atomic gas, exposed to a strong laser field, the collisional and Doppler broadenings are negligible in comparison with the ionization one, the off-diagonal decay rates can be calculated as $\gamma_{i,j} = (\gamma_j + \gamma_i)/2$. The initial and boundary conditions are

$$\begin{aligned} \tilde{E}(0,t) &= \tilde{E}_0 f(t) \\ \rho_{1s,1s}(x,0) &= 1 \\ \rho_{2s,2s}(x,0) &= 0, \\ \rho_{2p,2p}(x,0) &= 0, \\ \rho_{i,j}(x,0) &= 0, i \neq j, \end{aligned} \quad (11)$$

where $f(t)$ is an envelope of the incident XUV field. These equations are written and numerically solved in the basis of bare atomic states using a fourth-order Runge-Kutta scheme for time step and a second-order Adams-Bashforth scheme for steps in x [32].

Let us consider a propagation of an incident XUV pulse with carrier wavelength 59.16 nm and Gaussian envelope with FWHM 145 fs and peak intensity $I = 10^{10}$ W/cm² through the gas of helium with atomic density 10^{17} cm⁻³, irradiated by a 6176-nm IR field with intensity $I = 2.5 \times 10^{12}$ W/cm². The bandwidth of the incident XUV pulse is 0.01 eV, which is much less than the energy separation between the Floquet states, $\lambda_1 - \lambda_2 \approx 0.58\omega_{\text{IR}} \approx 0.12$ eV. The XUV field with such wavelength and pulse duration might be produced via the resonantly enhanced high-harmonic generation in an InP plasma plume [33,34]. Another way to generate it is frequency doubling of 355-nm radiation in a nonlinear crystal, followed by its frequency tripling in a gas. The time dependence of the output XUV intensity strongly depends on whether the output spectral component at the frequency of the incident XUV radiation is attenuated or not; see Fig. 5. In the presence of attenuation to the level of the generated sidebands the well-shaped pulses with duration 2 fs and peak intensity, equal to 0.87 maximum intensity of the incident XUV radiation, are produced at the output of the medium with the *optimal* propagation length 4.00 mm; see Fig. 5(a). It is worth noting that an optical thickness, defined as a ratio of medium length to characteristic length at which an intensity of the resonant field is decreased by $e \approx 2.718$ times, in the medium of IR-dressed atoms is smaller than in the unperturbed medium. Namely, the additional multiplier $a_2^{1,2p} \sum_{m \neq 0} a_{2m}^{1,2p} \exp(-2im\omega_{\text{IR}}\tau)$ appears in (7). Thus the effective optical thickness for a perturbed medium might be roughly estimated as $2|a_2^{1,2p}|^2 \frac{2\pi\omega_X N |d_{2p,1s}|^2}{c\hbar\gamma_{1s,2p}}$. For the considered parameters of the medium and the IR field, it is equal to 0.87. Under these conditions, the efficiency of transformation, defined as a ratio of the incident XUV radiation energy to the energy contained in the pulse train, equals 19.3%. For shorter propagation lengths a form of pulses is almost identical, while their intensity (and, thus, the

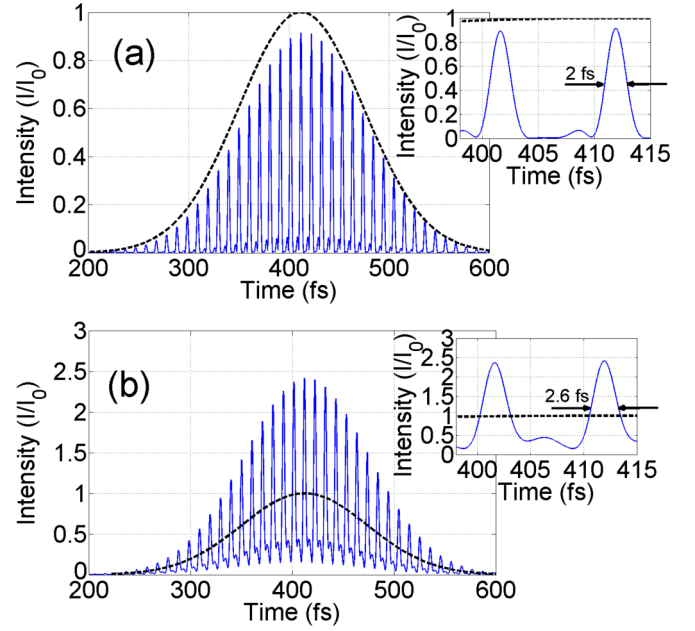


FIG. 5. (a) The XUV pulse at the entrance to the medium (black dashed line) and after propagation through 4 mm of helium gas with atomic density 10^{17} cm⁻³ irradiated by a 6176-nm IR field with intensity $I = 2.5 \times 10^{12}$ W/cm² (blue solid line). The resonant component of the output XUV radiation (corresponding to the incident field) is attenuated to the level of adjacent sidebands. Inset: a couple of pulses from the train shown in the main figure. (b) The same as in (a), but the resonant XUV spectral component is not attenuated.

transformation efficiency) is smaller. For longer propagation distances, the peak intensity of the produced pulses is no longer increasing, while their duration becomes larger. In the absence of attenuation, both the peak pulse intensity and the efficiency of transformation are substantially increased at the cost of increased pulse duration and pedestal. Thus, for the same parameters of the incident XUV and IR fields and the medium in the absence of attenuation the peak intensity of the pulses is 2.7 times larger than the peak intensity of the incident XUV radiation, while the efficiency of transformation reaches 80.6%; see Fig. 5(b).

V. SCALING TO OTHER ATOMIC SYSTEMS

The suggested method is easily scalable to an arbitrary three-level system with one high-frequency (say, XUV) dipole-allowed transition and one low-frequency (say, IR) dipole-allowed transition. Such a scalability potentially allows adjusting the carrier frequency and duration of the produced pulses of XUV radiation via the proper choice of the generating medium. Let us consider an atomic system with some IR transition with frequency ω_{23} . Choosing the frequency and the amplitude of the IR field according to the criteria presented in Sec. II, that is, $\omega_{\text{IR}}/\omega_{23} = 1/3$ and $\tilde{E}_{\text{IR}}d_{2,3}/\omega_{23} \approx 1.11$, leads to the creation of Floquet states with the same coefficients $a_{i;\alpha_0}^m$ as in Sec. II and allows pulse train formation from the resonant XUV radiation. Suppose we choose three-level atoms with IR transition frequency X times bigger than the $2s2p$ transition in He and set the frequency and the Rabi frequency

of the IR field to be X times bigger as well (the incident XUV radiation frequency has to be properly adjusted). In this case, the sideband separation, $2\omega_{\text{IR}}$, will also be X times bigger than in the case of He atoms, which means that the duration of the pulses (as well as the repetition period) will be X times smaller. It opens up the possibility for efficient conversion of an XUV radiation into a train of subfemtosecond pulses.

Let us consider, for example, Li+ ions. The energy-level diagram of the Li+ ion is the same as for helium, but the transition wavelengths for $1s^2 \leftrightarrow 1s2p$ and $1s2s \leftrightarrow 1s2p$ transitions are 19.928 and 958.4 nm, correspondingly. The other relevant parameters of Li+ ions can be found in [35]. It is worth noting that a 19.9-nm Li+-based x-ray laser was theoretically suggested and investigated [36–38]. An emission at 19.9 nm was experimentally observed from lithium plasma XUV sources [39,40]. Applying the described scaling approach, we immediately find the wavelength and intensity of the IR field, required for the ultrashort pulses formation, which are $3 \times 958.4 \sim 2875$ nm and $I = 4.4 \times 10^{13}$ W/cm², respectively. Using the Floquet approach, we find that the XUV field resonant to the first Floquet state has a wavelength of 20.1 nm. In order to estimate an efficiency of transformation of the XUV radiation into the pulse train we simulate propagation of both XUV and IR fields in an optically thick Li+ plasma layer taking into account the plasma dispersion, as well as the collisional broadening of the relevant transition lines. The plasma dispersion for the IR field is taken into account in Eq. (10) by replacing $\cos(\omega_{\text{IR}}\tau)$ with $\cos[\omega_{\text{IR}}(t - xn_{\text{plasma}}/c)]$, where $n_{\text{plasma}} = \sqrt{1 - \omega_p^2/\omega_{\text{IR}}^2}$ is the plasma refractive index, ω_p is the plasma frequency; the plasma dispersion for the XUV field is negligible. For the typical temperature and concentration of plasma ~ 5000 K and 10^{18} cm⁻³, the linewidths γ_{1s2p} , γ_{1s2s} , γ_{2s2p} are mainly determined by collisional broadening and are in the range of a few meV [41,42]. Since the ionization potentials of $1s2s$ and $1s2p$ states are much higher in Li+ than in He (while the required intensity of the IR field is just an order of magnitude higher), a contribution of the ionization rates is negligible. As it follows from the numerical solution of Eq. (10), at the output of the medium with the length of 80 μm (which corresponds to the effective optical thickness $2|a_2^{1,2p}|^2 \frac{2\pi\omega_X N |d_{2p,1s}|^2}{c\hbar\gamma_{1s,2p}} \approx 3.9$), a train of pulses will be produced with the pulse duration of 0.99 fs (which is remarkably close to the prediction of the scaling law, $2 \text{ fs} \times 2875/6176 \approx 0.93 \text{ fs}$); see Fig. 6. The efficiency of transformation into the pulse train equals 26.6%. The output pulses are delayed with respect to the incident one due to the resonant dispersion of Li+ ions, which turns out to be important, since the bandwidth of the incident XUV radiation exceeds the linewidth of the resonant transition $1s^2 \leftrightarrow 1s2p$. Similar to the case of He atoms, without attenuation of the resonant output XUV spectral component both the peak pulse intensity and the efficiency of transformation are substantially increased at the cost of increased pulse duration and pedestal. Thus, for the same parameters of the medium in the absence of attenuation the peak intensity of the pulses is 2 times larger than the peak intensity of the incident XUV field, while efficiency of transformation reaches 87.4%; see Fig. 6(b).

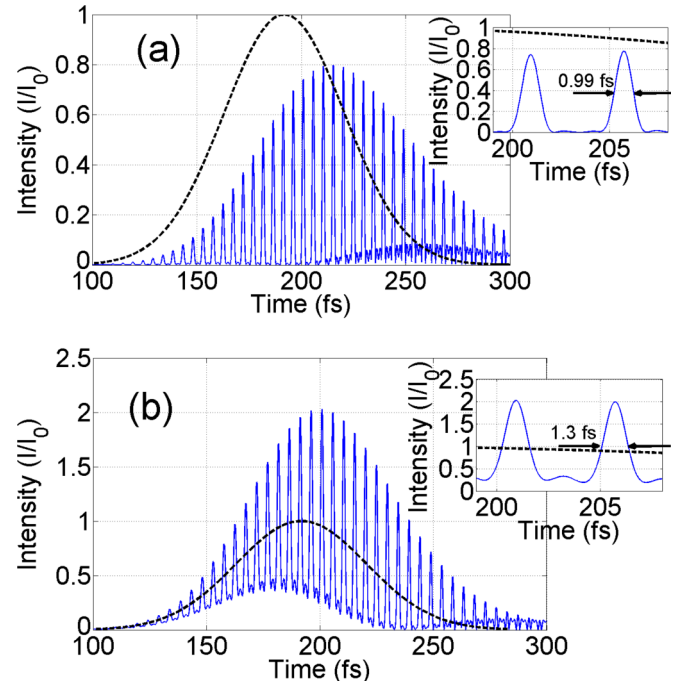


FIG. 6. Intensity of the 20.1-nm XUV field at the entrance to the medium (black dashed line) and after propagation through 80 μm of Li+ plasma along with a 2875-nm IR field with intensity $I = 4.4 \times 10^{13}$ W/cm² (blue solid line). (a) The resonant frequency of the XUV field at the exit of the medium is attenuated. Ion density is 10^{18} cm⁻³. Inset: a couple of the pulses from the train shown in the main figure. (b) The same as (a), but the resonant XUV spectral component is not attenuated.

VI. CONCLUSION

In the present paper, we have shown the possibility to produce the ultrashort femtosecond and subfemtosecond pulses of XUV radiation via its resonant interaction with the medium of IR-field-dressed non-hydrogen-like atoms. The mechanism of pulses formation is based on mixing and modulating of the excited atomic states by the nonionizing relatively low-frequency IR field. Using Floquet formalism within the three-level model of He atoms and He-like Li+ ions, we found the optimal parameters (frequency and amplitude) of the IR field, providing formation of well-shaped pulses with duration 2 fs and 990 as, correspondingly. We verified that the presence of the other bound atomic states and ionization results in only slight changes in the shape of produced pulses. We found a simple scalability law which can be used for determination of the optimal parameters of the IR field providing the ultrashort pulses formation in various non-hydrogen-like media under conditions when the three-level model approximation is applicable. Under the optimal conditions, the efficiency of pulses formation reaches 80%–90%, which makes the suggested technique very favorable for time shaping of picosecond pulses of x-ray lasers. Since this method does not imply ionization either from the ground, or from the excited states of the generating medium, it can be potentially used directly in the active media of x-ray lasers.

ACKNOWLEDGMENTS

The research was supported by the National Science Foundation (NSF) Grants No. PHY-1307346 and No. PHY-1506467. The authors acknowledge Texas A&M High Performance Research Computing for the use of supercomputer time. T.R.A. gratefully acknowledges the support by Herman F. Heep and Minnie Belle Heep Texas A&M University Endowed

Fund held and administrated by Texas A&M Foundation. V.A.A. acknowledges support by RFBR under Grants No. 16-32-60173, No. 16-02-01034, No. 16-02-00527, No. 14-02-00762, No. 14-29-07152, and No. 14-22-02034, as well as a personal grant for young scientists from the Grant Council of the President of Russian Federation and a personal grant for young scientists from Dynasty Foundation.

-
- [1] A. Cavalleri, M. Rini, H. H. W. Chong, S. Fourmaux, T. E. Glover, P. A. Heimann, J. C. Kieffer, and R. W. Schoenlein, *Phys. Rev. Lett.* **95**, 067405 (2005).
- [2] K. Hoffmann, B. Murphy, B. Erk, A. Helal, N. Kandadai, J. Keto, and T. Ditmire, *High Energy Density Phys.* **6**, 185 (2010).
- [3] L. Yue and L. B. Madsen, *Phys. Rev. Lett.* **115**, 033001 (2015).
- [4] S. Mathias, M. Bauer, M. Aeschlimann, L. Miaja-Avila, H. C. Kapteyn, and M. M. Murnane, in *Dynamics at Solid State Surfaces and Interfaces: Current Developments*, Volume 1, edited by U. Bovensiepen, H. Petek and M. Wolf (Wiley-VCH Verlag GmbH & Co. KGaA, Weinheim, Germany, 2010), pp. 501–535.
- [5] C. Ott, A. Kaldun, P. Raith, K. Meyer, M. Laux, J. Evers, C. H. Keitel, C. H. Greene, and T. Pfeifer, *Science* **340**, 716 (2013).
- [6] D. Fabris, T. Witting, W. A. Okell, D. J. Walke, P. Matia-Hernando, J. Henkel, T. R. Barillot, M. Lein, J. P. Marangos, and J. W. G. Tisch, *Nat. Photonics* **9**, 383 (2015).
- [7] P. M. Paul, E. S. Toma, P. Breger, G. Mullot, F. Auge, Ph. Balcou, H. G. Muller, and P. Agostini, *Science* **292**, 1689 (2001).
- [8] T. Popmintchev, M. C. Chen, D. Popmintchev, P. Arpin, S. Brown, S. Alisauskas, G. Andriukaitis, T. Balciunas, O. D. Mücke, A. Pugzlys, A. Baltuska, B. Shim, S. E. Schrauth, A. Gaeta, C. Hernández-García, L. Plaja, A. Becker, A. Jaron-Becker, M. M. Murnane, and H. C. Kapteyn, *Science* **336**, 1287 (2012).
- [9] K. Zhao, Q. Zhang, M. Chini, Y. Wu, X. Wang, and Z. Chang, *Opt. Lett.* **37**, 3891 (2012).
- [10] M.-C. Chen, P. Arpin, T. Popmintchev, M. Gerrity, B. Zhang, M. Seaberg, D. Popmintchev, M. M. Murnane, and H. C. Kapteyn, *Phys. Rev. Lett.* **105**, 173901 (2010).
- [11] D. Popmintchev, C. Hernández-García, F. Dollar, C. Mancuso, J. A. Pérez-Hernández, M.-C. Chen, A. Hankla, X. Gao, B. Shim, A. L. Gaeta, M. Tarazkar, D. A. Romanov, R. J. Levis, J. A. Gaffney, M. Foord, S. B. Libby, A. Jaron-Becker, A. Becker, L. Plaja, and M. M. Murnane, *Science* **350**, 1225 (2015).
- [12] S. Schreiber, in *Proceedings, 33rd International Free Electron Laser Conference (FEL 2011): Shanghai, China, August 22–26, 2011*, edited by Z. Zhao and D. Wang (SINAP, Shanghai, China, 2012), pp. 164–165.
- [13] W. Ackermann *et al.*, *Nat. Photonics* **1**, 336 (2007).
- [14] C. Pellegrini *et al.*, *Nucl. Instrum. Methods Phys. Res., Sect. A* **331**, 223 (1993).
- [15] SPring-8-II conceptual design report, (Riken SPring-8 Center, Harima, Hapan, 2014).
- [16] B. A. Reagan, M. Berrill, K. A. Wernsing, C. Baumgarten, M. Woolston, and J. J. Rocca, *Phys. Rev. A* **89**, 053820 (2014).
- [17] P. W. Wachulak, A. Bartnik, H. Fiedorowicz, P. Rudawski, R. Jarocki, J. Kostecki, and M. Szczyrek, *Nucl. Instrum. Methods Phys. Res., Sect. B* **268**, 1692 (2010).
- [18] D. V. Korobkin, C. H. Nam, S. Suckewer, and A. Goltsov, *Phys. Rev. Lett.* **77**, 5206 (1996).
- [19] Y. V. Radeonychev, V. A. Polovinkin, and Olga Kocharovskaya, *Phys. Rev. Lett.* **105**, 183902 (2010).
- [20] V. A. Polovinkin, Y. V. Radeonychev, and Olga Kocharovskaya, *Opt. Lett.* **36**, 2296 (2011).
- [21] V. A. Antonov, Y. V. Radeonychev, and O. Kocharovskaya, *Phys. Rev. A* **88**, 053849 (2013).
- [22] V. A. Antonov, Y. V. Radeonychev, and O. Kocharovskaya, *Phys. Rev. Lett.* **110**, 213903 (2013).
- [23] V. A. Antonov, T. R. Akhmedzhanov, Y. V. Radeonychev, and Olga Kocharovskaya, *Phys. Rev. A* **91**, 023830 (2015).
- [24] S. I. Chu and D. A. Telnov, *Phys. Rep.* **390**, 1 (2004).
- [25] M. Chini, X. Wang, Y. Cheng, Y. Wu, D. Zhao, D. A. Telnov, S. I. Chu, and Z. Chang, *Sci. Rep.* **3**, 1105 (2013).
- [26] S. H. Autler and C. H. Townes, *Phys. Rev.* **100**, 703 (1955).
- [27] T. R. Akhmedzhanov, V. A. Antonov, and Olga Kocharovskaya, (unpublished).
- [28] N. Kaiser, S. Yulin, M. Perske, and T. Feigl, *Proc. SPIE* **7101**, 71010Z (2008).
- [29] S. A. Bogachev, N. I. Chkhalo, S. V. Kuzin, D. E. Pariev, V. N. Polkovnikov, N. N. Salashchenko, S. V. Shestov, and S. Y. Zuev, *Appl. Opt.* **55**, 2126 (2016).
- [30] X.-M. Tong and S.-I. Chu, *Chem. Phys.* **217**, 119 (1997).
- [31] P.-C. Li, C. Laughlin, and Shih-I Chu, *Phys. Rev. A* **89**, 023431 (2014).
- [32] G. Demeter, *Comput. Phys. Commun.* **184**, 1203 (2012).
- [33] R. A. Ganeev, H. Singhal, P. A. Naik, V. Arora, U. Chakravarty, J. A. Chakera, R. A. Khan, I. A. Kulagin, P. V. Redkin, M. Raghuramaiah, and P. D. Gupta, *Phys. Rev. A* **74**, 063824 (2006).
- [34] R. A. Ganeev, *High-order Harmonic Generation in Laser Plasma Plumes* (Imperial College Press, London, 2013), p. 46.
- [35] W. L. Wiese and J. R. Fuhr, *J. Phys. Chem. Ref. Data* **38**, 565 (2009).
- [36] P. L. Shkolnikov and A. E. Kaplan, *J. Opt. Soc. Am. B* **9**, 2128 (1992).
- [37] K. Lan, E. E. Fill, and J. Meyer-ter-Vehn, *Europhys. Lett.*, **64**, 454 (2003).
- [38] K. E. Lan, E. E. Fill, and J. Meyer-ter-Vehn, *Laser Part. Beams* **22**, 261 (2004).
- [39] Y. Nagata, K. Midorikawa, S. Kubodera, M. Obara, H. Tashiro, and K. Toyoda, *Phys. Rev. Lett.* **71**, 3774 (1993).
- [40] S. A. George, W. Silfvast, K. Takenoshita, R. Bernath, C.-S. Koay, G. Shimkaveg, and M. Richardson, *Proc. SPIE* **6151**, 615143 (2006).
- [41] M. S. Dimitrijevic and S. Sahal-Bréchet, *Phys. Scr.* **54**, 50 (1996).
- [42] N. Konjevic, *Phys. Rep.* **316**, 339 (1999).